Chemical Science

ROYAL SOCIETY OF CHEMISTRY

EDGE ARTICLE

View Article Online
View Journal | View Issue

Cite this: *Chem. Sci.*, 2025, **16**, 16180

All publication charges for this article have been paid for by the Royal Society of Chemistry

Controlling molecular machines *via* optimally oriented external electric fields

Marco Severi, *[a] Ibério de P. R. Moreira, [bc] Jordi Ribas-Ariño, [bc] Wolfgang Quapp [d] and Josep Maria Bofill [ce]

The rectification of Brownian motion allows the operation of molecular machines, enabling them to perform directed tasks in biological and synthetic systems. Among the various control strategies, electric fields (E-fields) are emerging as a powerful means to modulate this rectification. Here, we demonstrate E-field-driven control of molecular motion in two representative molecular machines – a fluorene-based overcrowded alkene and an achiral rotor model – that operate *via* distinct mechanisms. Furthermore, we identify the optimal orientation of the applied E-fields that transforms activated steps into effectively barrierless processes, achieving directional control of internal molecular motion with minimal field strength. This is computationally demonstrated using our recently introduced polarizable molecular electric dipole model, which predicts E-fields to induce coalescence of transition states and energy minima on potential energy surfaces. Specifically, our studies show that E-fields enable bidirectional isomerization in the ground state without having to rely on photochemical processes that require energies much higher than the corresponding activation energy. Logical control over rotation, including the implementation of "STOP" and "GO" instructions, can also be achieved through E-field modulation without molecular chirality. Crucially, the required field strengths are within reach of current scanning tunneling microscope technology. Our results offer a generalizable, non-invasive design principle for the next generation of electric field-controlled molecular machines.

Received 1st July 2025
Accepted 4th August 2025

DOI: 10.1039/d5sc04835d

rsc.li/chemical-science

1 Introduction

The rectification of Brownian motion is a fundamental principle underlying the operation of molecular machines, which are essential for numerous biological processes.[1] Brownian motion, the random thermal movement of particles in a fluid, is typically nondirectional. However, in biological systems, mechanisms exist that rectify this stochastic motion, converting it into directed work. This principle is vital for cellular transport, enzymatic functions and force generation.[2] Molecular machines, such as motor proteins (*e.g.*, kinesin, myosin), harness rectified Brownian motion to perform these essential functions. Operating far from thermodynamic equilibrium, they utilize energy to bias random fluctuations in a preferred direction.[3] Understanding these mechanisms not only provides insight into fundamental biological processes but also informs the design of artificial molecular motors.

Advances in this field have driven major scientific breakthroughs, recognized by the 2016 Nobel Prize in Chemistry.[4–7] Today, synthetic molecular machines are capable of rectifying Brownian motion through external stimuli, enabling controlled molecular movement with significant potential in biomedical applications and smart materials design.[1,8–11] Just like macroscopic machines, synthetic molecular machines require fine-tuned control of molecular processes. To achieve this, researchers have developed strategies based on thermal isomerisation, coordination to metal ions,[1,12] redox and chemical reactions,[13,14] electric fields,[15] pH changes,[16] and hybrid systems that integrate biological components.[3]

Electric fields stand out as a superior method of control. Unlike chemical inputs, electric fields generate no waste and offer precise spatial and temporal control.[17] As a result, a wide array of molecular machines has been developed based on electric stimuli, including those driven by oscillating fields (light),[15,17–22] static fields,[23–27] alternating fields,[28,29] rotating fields,[30] and fields generated by scanning tunneling microscope (STM) tips.[31]

Molecular machines tethered to (supra)molecules, polymers, or surfaces are particularly important, as they constitute the building blocks for functional molecular materials and

[a]*Department of Chemistry G. Ciamician, University of Bologna, Via P. Gobetti 85, 40129 Bologna, Italy. E-mail: marco.severi6@unibo.it*

[b]*Departament de Ciència de Materials i Química Física, Secció de Química Física, Universitat de Barcelona, Martí i Franquès 1, 08028 Barcelona, Spain*

[c]*Institut de Química Teòrica i Computacional, (IQTCUB), Universitat de Barcelona, Martí i Franquès 1, 08028 Barcelona, Spain*

[d]*Mathematisches Institut, Universität Leipzig, D-04009 Leipzig, PF 100920, Germany*

[e]*Departament de Química Inorgànica i Orgànica, Secció de Química Orgànica, Universitat de Barcelona, Martí i Franquès 1, 08028 Barcelona, Spain*

devices.[32–34] Remarkably, Prezzi, Tour, Grill, and co-workers demonstrated the unidirectional motion of a molecular motor on a copper surface using an electric field from an STM tip,[35] while Shen, Wang, and Yang reviewed the use of molecular motors to control phases in soft materials.[36]

Simultaneously, theoretical understanding of rectification has progressed, with the energy ratchet and information ratchet emerging as key mechanisms.[37,38] Though they differ in detail, both rely on changes in the potential energy surface (PES) or excitation to higher electronic states to push the system out of equilibrium. As synthetic molecular machines are inspired by nature, the concept of using external electric fields to control molecular motion builds upon a rich foundation of earlier work in biological systems. Notably, the framework of electro-conformational coupling[39,40] demonstrated how a variation of a membrane potential of tens of mV generates strong electric fields that can bias the conformational states of membrane proteins and enzymes. The usage of external perturbations to control enzymes[41,42] finally stemmed in the concepts of information ratchet and energy ratchet.[43]

We recently developed a model that optimally drives systems out of equilibrium using external electric fields, with successful applications to chemical catalysis.[44–47] Our polarizable molecular electric dipole (PMED) model calculates the electric field needed to remove the energy barrier between reactants and transition states. In catalysis, this accelerates product formation; in molecular machines, it facilitates movement between states, *e.g.*: a shuttle that moves between two stations or a rotation around a bond. Though distinct in context, both cases involve activated processes that benefit from optimal external field control, which the PMED model provides (Fig. 1).

In this study, we apply the PMED model to two molecular machines. The first is an overcrowded alkene based on fluorene, previously studied by Feringa, Filatov, and collaborators.[48] We show that a carefully designed static electric field can eliminate the rotation barrier in the ground state, removing the need for photoexcitation. We also demonstrate that the field can induce isomerisation in the reverse direction, potentially disrupting the machine's unidirectional motion. Our approach offers a more general design principle, as it eliminates the reliance on conical intersections. The static field is designed to distort the ground state surface, removing the need of the conical intersection to speed up the isomerisation, simplifying the synthetic desing of the next generation of molecular motors. Additionally, the use of static fields avoids degradation and secondary processes, enhancing motor stability.

The second system is a symmetric analogue of rotary motors previously explored by Fujimura and colleagues.[49–52] While chirality often facilitates directionality, we focus on an achiral molecule with three potential energy minima, two of which are symmetrically equivalent. By applying an external electric field, we break this symmetry and selectively remove energy barriers, enabling controlled, directional motion. This approach grants full control over the rotor's behavior, allowing for clockwise rotation, anticlockwise rotation, or confinement in the central minimum. Each field breaks the PES symmetry, energetically distinguishing otherwise equivalent minima. In analogy to molecular shuttles,[53] this provides logical control over the rotor's motion, implementing "STOP" and "GO" instructions *via* external fields. In the absence of a field, thermal fluctuations drive symmetric Brownian motion across the three stations. However, applying the appropriate external field biases the system toward a specific minimum, effectively rectifying the motion.

Importantly, the computed field amplitudes required to achieve this directional control are well within the capabilities of current STM technology.[54–56] STM tips can generate the necessary electric fields to induce these effects, offering a practical and feasible means for precise manipulation of molecular machines.

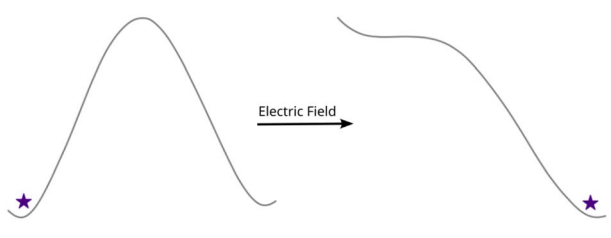

Fig. 1 Schematic of the PMED model. Based on the optimal bond-breaking point (oBBP), it computes an external electric field that removes a reaction barrier and isolates an energy minimum. The star denotes the initial and final system states.

2 Methods

For the purpose of this work it is sufficient to briefly review the key aspects of the PMED model and we refer the interested reader to ref. 46, which describes the latest version of the PMED model. The PMED model is based on optimal control and catastrophe theories. First, using catastrophe theory, it locates a special point between the reactants and the transition state in which these two stationary points can coalesce upon the action of an external perturbation; second, using optimal control theory, it computes the optimal external electric field, both in direction and intensity, to actually make them coalesce. The annihilation of these two stationary points into one results in the removal of the energy barrier between the reactants and products. The point in which the reactants and the transition state coalesce is called optimal bond-breaking point (oBBP), it is a special point of the PES where the gradient is an eigenvector of the hessian, member of the family of the gradient extremal points.[57,58] The oBBP has optimal properties[59–61] from which it follows the calculation of the optimal external electric field.

The hypothesis of the PMED model is that the PES under the effect of an external electric field can be described with the expression

$$V_{\mathbf{e}_n}(\mathbf{x}, E) = V(\mathbf{x}) - E\mathbf{e}_n{}^T\left[\mathbf{d}(\mathbf{x}) + \frac{1}{2}\mathbf{A}(\mathbf{x})E\mathbf{e}_n\right] \quad (1)$$

where $V(\mathbf{x})$ is the original or unperturbed PES, $\mathbf{d}(\mathbf{x})$ is the dipole moment vector and $\mathbf{A}(\mathbf{x})$ is the polarizability matrix. $\mathbf{x}$ is the variable or the set of variables used to construct the PES, so it

can be any variable(s) used to describe the chemical process of interest, *e.g.* a distance, an angle, a dihedral.

On the surface, we can define an optimal bond-breaking point (oBBP) that lies somewhere in between a minimum and a transition state and follows the conditions

$$\mathbf{H}(\mathbf{x}_{\mathrm{oBBP}})\mathbf{g}(\mathbf{x}_{\mathrm{oBBP}}) = 0 \quad (2)$$

$$\mathbf{g}(\mathbf{x}_{\mathrm{oBBP}}) \neq 0 \quad (3)$$

$\mathbf{H}(\mathbf{x}_{\mathrm{oBBP}})$ is the Hessian of the original PES at the oBBP and $\mathbf{g}(\mathbf{x}_{\mathrm{oBBP}})$ is the gradient of the original PES at the oBBP. A point that, in general, satisfies these conditions is a gradient extremal point. It should be noted that the oBBP is a point of the border of a concavity zone. The reactant minimum is in a concavity zone of the potential surface. Normally, the oBBP is located halfway between the reactant minimum and the transition state. After the location of the oBBP, the optimal external electric field can be determined by imposing two conditions: (i) the Hessian matrix of the perturbed PES must be equal to the Hessian matrix of the original PES at the oBBP; (ii) the gradient of the original PES is an eigenvector of the Hessian matrix of the PES pertubed by the electric field. Once applied the field computed with the PMED model, the barrier between the oBBP and the transition state and the barrier between the oBBP and the reactant minimum are removed. This results in a barrierless path between the reactants and the products, therefore the process requires no thermal energy (see Fig. 1).

The potential energy surfaces (PES) of both systems were computed by means of quantum chemical calculations. The PES scans were performed using the ORCA 5.0.3 program system,[62] employing the B3LYP functional[63–65] and the 'minimally-augmented'-def2-SVP basis set.[66,67] All calculations included the D3BJ dispersion correction.[68,69] The DFT calculations were carried out using the RIJCOSX approximation, which is the default for hybrid functionals in ORCA.[70–72] The PES were obtained through so-called relaxed scans, in which the scanned degrees of freedom were constrained while the remaining ones were optimized. For each point on the PES, the electronic energy, dipole moment, and polarizability were computed. The algorithm for the location of the oBBPs and the calculation of the electric fields is described in ref. 46 and implemented in the MANULS program, freely available on GitHub (**https://github.com/MSeveri96/MANULS**).[73]

3 Results

3.1 Fluorene molecular motor

We start by considering a molecular rotary motor derived from a chiral overcrowded alkene, 9-(2,4,7-trimethyl-2,3-dihydro1*H*-inden-1-ylidene)-9*H*-fluorene.[48] This class of motors operates through two consecutive photochemical and thermal steps. The photochemical step is the *E*–*Z* photoisomerisation of the central double bond. The thermal step is an helix inversion that changes the elicity of the molecule from P to M or *vice versa*.[19] This leads to four stable conformations throughout the motor cycle. Light is used to fuel the rotation because the *E*–*Z* isomerisation is thermally inaccessible, whereas helix inversion typically occurs spontaneously.

Here, we focus exclusively on the photoisomerisation step, demonstrating that a properly oriented static electric field can catalyse the *E*–*Z* isomerisation without requiring excitation to a higher electronic state. Thus, we consider only two isomers, labeled P and M for simplicity, as shown in Fig. 2, without using the full *E*/*Z* nomenclature.

The PES of the ground state has been thoroughly studied in ref. 48. Following the same approach, we scan two key angles: θ, which describes the rotation around the central double bond, and α, which captures the pyramidalisation of one of the carbon atoms involved in this bond. To define an internal frame of reference, we introduce two vectors: a vertical vector (v_{v}) aligned with the central double bond and a horizontal vector (v_{h}) indicating the orientation of the fluorene moiety. This frame allows us to express the optimal direction of the external electric field relative to the molecular orientation (see Fig. 3).

By scanning the angle θ and α, we identify the PES minima corresponding to the P and M isomers, as well as the transition state, found at $\theta = 95°$ and $\alpha = 0°$ on our grid (Fig. 4a).

Once constructed the PES, we investigate the isomerisation from P to M. Using the MANULS code we locate the optimal BBP in which the transition state (TS) and the P minimum coalesce. The oBBP associated with the P to M isomerisation can be found at $\theta = 60°$ and $\alpha = 0°$. From the properties of the oBBP we compute an external electric field that lowers the isomerisation barrier from 24 kcal mol^{-1} to just 1.6 kcal mol^{-1} (Fig. 4b). This field has an amplitude of 1.40 V Å^{-1}. Its direction, relative to the molecular frame, forms angles of 138° with v_{v} and 125° with v_{h} (purple arrow in Fig. 4d).

The electric field strength reported here (1.40 V Å^{-1}) is higher than the 500 mV bias used to drive motion in molecular motors on Cu(111) surfaces, as demonstrated by Feringa and collaborators in ref. 74. This discrepancy arises from the fundamentally different mechanisms involved. In Feringa's work, directional motion is achieved *via* transient electronic excitation, that is population of the LUMO through inelastic electron tunnelling, which facilitates isomerization in a manner akin to photoisomerization. In contrast, our approach does not rely on excitation but instead modifies the ground state potential energy surface directly using a uniform static electric field. This method eliminates the need for designing systems with conical intersections and avoids photochemical side reactions. It must

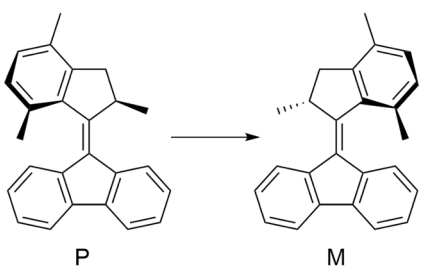

Fig. 2 Representation of the fluorene-based molecular motor, along with the nomenclature.

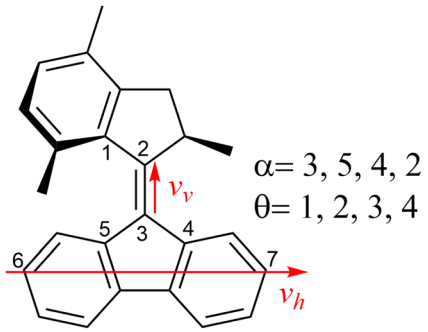

Fig. 3 Dihedral angles used to compute the PES and frame of reference employed. The vertical vector v_v is defined as the unit vector connecting the atoms 2 and 3. The horizontal vector v_h defines the directionality of the fluorene moiety and is defined as the unit vectors connecting the atoms 6 and 7.

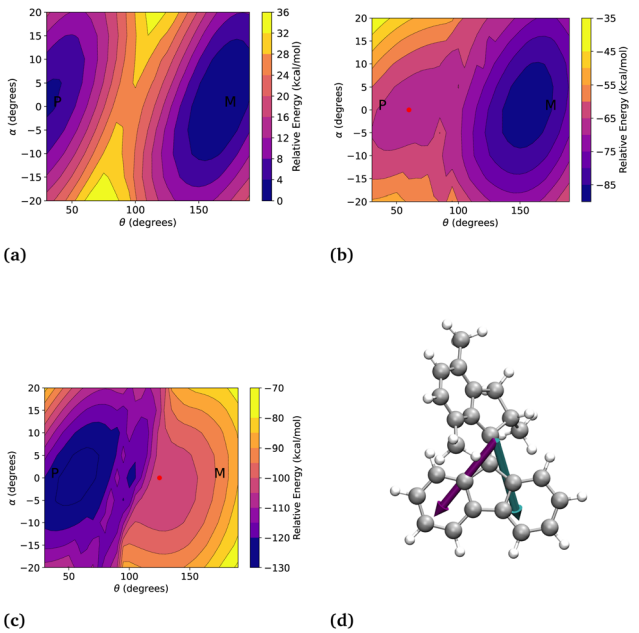

Fig. 4 (a) PES sectiom without the effect of the external electric field. (b) PES section under the effect of the field that eases the rotation from P to M. Corresponding oBBP in red. (c) PES section under the effect of the field that eases the rotation from M to P. Corresponding oBBP in red. (d) Molecular 3D structure with the direction of the computed external electric fields. Purple: field that catalyses the P to M isomerisation, cyan: field that catalyses the M to P isomerisation.

be kept in mind that the action of the electric field modifies the potential surface in such a way that if there are conic intersections, these are eliminated or are in an area of the potential surface far from the one we are interested in. The distinct mode of action naturally results in a different required field strength.

We then extend the analysis to the reverse rotation, from M to P. The oBBP is found at $\theta = 125°$ and $\alpha = 0°$. An electric field of 1.72 V Å^{-1} fully eliminates the 22.9 kcal mol^{-1} isomerisation barrier from M to P (Fig. 4c). This field makes angles of 140° with v_v and 105° with v_h (cyan arrow in Fig. 4d). Notably, the two fields are nearly symmetric with respect to the central double bond.

This molecular motor is engineered for unidirectional rotation from P to M, initiated by photoexcitation to the first excited state and followed by relaxation *via* a conical intersection.[48] The unidirectionality arises from the asymmetric shape of the PES in both the ground and excited states. While unidirectional motion is a key feature of molecular motors, our results demonstrate that – if needed – an external electric field can reshape the ground state PES to enable isomerization in the reverse direction.

3.2 Achiral rotor

In Section 3.1, we examined an intrinsically unidirectional molecular motor and demonstrated that an external electric field can both facilitate its rotation and reverse its direction. Here, we consider cyclopenta-2,4-diene-1-carbaldehyde, an achiral molecular rotor derived from the chiral motors extensively investigated theoretically by Fujimura and co-workers.[49–52]

We analyse the torsional motion around the central C–C bond (Fig. 5). The absence of chirality removes asymmetry from the PES, resulting in a symmetric energy landscape. Starting from the global minimum (G-MIN, torsional angle = 0°), both clockwise (CW) and anticlockwise (ACW) rotations lead to equivalent paths on the PES. Each direction involves a path to transition state (TS-CW or TS-ACW), descent into a local minimum (MIN-CW or MIN-ACW), and finally arrival at a symmetric transition state (SYM-TS) after a 180° rotation. The section of the PES, shown in Fig. 6a, is periodic over the interval −180° to +180°, with positive angles denoting ACW rotation.

Despite its simplicity, this system serves as a minimal model for a three-station molecular shuttle, with two degenerate side stations and a central global minimum.[75] Under thermal equilibrium, Brownian motion allows population of all minima according to the Maxwell–Boltzmann distribution, eliminating net directionality. Several strategies have been proposed to rectify thermal motion in such degenerate systems.[53,75] Here, we show that applying a static electric field can remove this degeneracy by stabilizing one minimum, thus shifting the equilibrium and enabling directional motion.

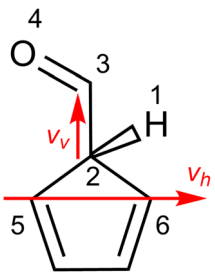

Fig. 5 Dihedral angle used to compute the PES and frame of reference employed. The torsional angle scanned to obtain the PES is defined by atoms 1–4. The vertical vector v_v is defined as the unit vector connecting the atoms 2 and 3. The horizontal vector v_h is defined as the unit vectors connecting the atoms 5 and 6, it describes the position of the cyclopentadiene with respect to the aldeyde.

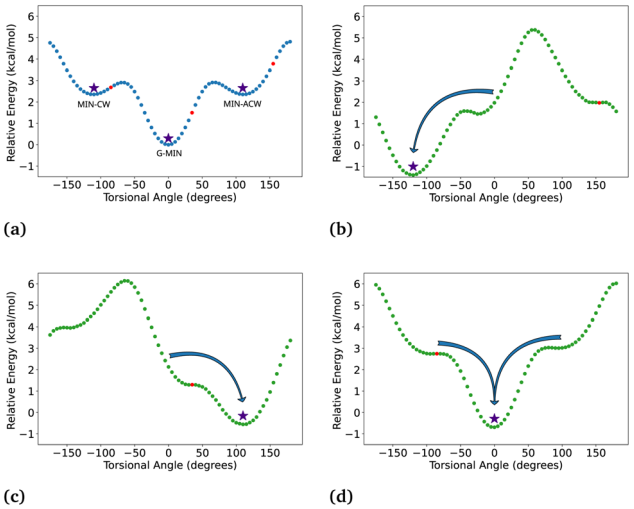

Fig. 6 (a) Unperturbed PES. (b) PES under a field promoting CW rotation (G-MIN to MIN-CW). (c) PES under a field stabilizing G-MIN and removing the side minima. (d) PES under a field promoting ACW rotation (G-MIN to MIN-ACW). Red dots denote oBBPs used to compute electric fields; purple stars highlight stabilized minima; arrows guide the visual interpretation of rotation.

Following the methodology described in Section 3.1, we use the internal coordinate frame defined by ν_v and ν_h (Fig. 5) to orient the electric field and evaluate its effects on the PES (Fig. 6).

Assuming that the system is initially localized at G-MIN, we first identify a field that promotes clockwise rotation by stabilizing MIN-CW and removing the barrier from G-MIN. This field has a magnitude of 0.40 V Å^{-1}, forms a 95° angle with ν_v, and a 132° angle with ν_h (Fig. 6b). Analogously, we compute a field that induces anticlockwise rotation, converting G-MIN into MIN-ACW. This field has a magnitude of 0.42 V Å^{-1}, with orientation angles of 113° relative to ν_v and 38° relative to ν_h (Fig. 6c). Finally, we identify a field that stabilizes G-MIN while eliminating both side minima, effectively halting the motion. This field has a magnitude of 0.12 V Å^{-1}, with angles of 116° and 97° relative to ν_v and ν_h, respectively (Fig. 6d).

Together, these three fields provide full control over the rotor's behavior: clockwise rotation, anticlockwise rotation, and confinement in the central minimum. Each field breaks the PES symmetry, energetically distinguishing otherwise equivalent minima. In analogy to molecular shuttles,[53] this enables logical control over motion, implementing "STOP" and "GO" instructions *via* external fields. In the absence of a field, thermal fluctuations drive symmetric Brownian motion across the three stations. Application of the appropriate field biases the system toward a specific minimum, effectively rectifying the motion. To achieve full rotation, the fields can be very slowly modulated out-of-phase with one another, subsequently populating the minima of the potential energy surface. With this procedure, the efficiency can approach 100%.[76] For example, starting from G-MIN, the molecule can be selectively driven to MIN-CW using the first field, returned to G-MIN with the second, and subsequently directed to MIN-ACW with the third. Releasing the field restores thermal motion, allowing the system to repopulate G-MIN and restart the sequence.

4 Conclusions

This work establishes that static external electric fields offer a powerful, tunable means of reshaping potential energy surfaces to modulate the dynamics of molecular machines with a high degree of precision. By leveraging the Polarizable Molecular Electric Dipole (PMED) model, we systematically identify fields that lower or entirely eliminate isomerisation barriers, thereby transforming otherwise activated processes into nearly barrierless transitions. Crucially, this is achieved without resorting to chemical modifications or the continuous input of photons.

In the case of the fluorene-based overcrowded alkene, our calculations show that electric fields can catalyse the ground state isomerisation typically driven by light. Remarkably, the electric-field-induced *E–Z* isomerization proceeds with energy inputs comparable to the intrinsic ground-state barrier, thereby avoiding the excess energy typically associated with electronic excitation and minimizing the risk of parasitic side reactions. This simplifies the design and synthesis of next-generation molecular motors by removing the requirement for photoactive excited state and conical intersection and also mitigates issues such as photodegradation, allowing for increased longevity and operational stability. Furthermore, the ability to reverse the direction of rotation *via* tailored electric fields challenges the conventional paradigm of irreversible unidirectional molecular motion.

For the achiral rotor, we demonstrated that symmetry-breaking *via* static electric fields enables selective, directional control over molecular rotation. The field-dependent modulation of the potential energy surface introduces logical functionality ("GO", "STOP") akin to that seen in switchable molecular shuttles. This level of control could be instrumental for implementing logic gates at the molecular level or for powering nanoscale devices.

Importantly, all electric fields computed in this study fall within experimentally achievable ranges using STM tips, affirming the practical feasibility of the approach. The PMED model thus serves as a predictive design tool that bridges quantum chemical theory with experimental implementation.

Author contributions

Marco Severi: conceptualization (equal); data curation (lead); formal analysis (equal); investigation (equal); methodology (equal); resources (equal); software (lead); validation (equal); visualization (lead); writing – original draft (lead); writing – review & editing (lead). Ibério de P. R. Moreira: conceptualization (equal); data curation (supporting); formal analysis (supporting); investigation (equal); methodology (equal); resources (equal); validation (supporting); visualization (equal); writing – original draft (equal); writing – review & editing (equal). Jordi Ribas-Ariño: conceptualization (equal); data curation (supporting); formal analysis (supporting); investigation (equal);

methodology (equal); resources (equal); validation (supporting); visualization (equal); writing – original draft (equal); writing – review & editing (equal). Wolfgang Quapp: conceptualization (equal); data curation (supporting); formal analysis (supporting); investigation (equal); methodology (equal); resources (equal); validation (supporting); visualization (equal); writing – original draft (equal); writing – review & editing (equal). Josep Maria Bofill: conceptualization (equal); data curation (supporting); formal analysis (supporting); investigation (equal); methodology (equal); resources (equal); validation (supporting); visualization (equal); writing – original draft (equal); writing – review & editing (equal).

Conflicts of interest

There are no conflicts to declare.

Data availability

The MANULS code for the calculation of the electric fields can be found at **https://github.com/MSeveri96/MANULS**. The version of the code employed for this study is version 1.0.

Acknowledgements

Josp Maria Bofill acknowledges the Spanish Ministerio de Ciencia, Innovación y Universidades, the Spanish Structures of Excellence María de Maeztu program through Grant No. CEX2021-001202-M. This work was supported by Agència de Gestió d'Ajuts Universitaris i de Recerca of Generalitat de Catalunya, Project No. 2021SGR00354. Jordi Ribas-Ariño acknowledges the financial support from the Spanish Ministerio de Ciencia, Innovación y Universidades and Agencia Estatal de Investigación (AEI) MCIN/AEI/10.13039/501100011033 through project PID2023-149691NB-I00.

References

1 R. Iino, K. Kinbara and Z. Bryant, *Chem. Rev.*, 2020, **120**, 1–4.
2 J. Robert-Paganin, O. Pylypenko, C. Kikuti, H. L. Sweeney and A. Houdusse, *Chem. Rev.*, 2020, **120**, 5–35.
3 G. Saper and H. Hess, *Chem. Rev.*, 2020, **120**, 288–309.
4 J.-P. Sauvage, *Angew. Chem., Int. Ed.*, 2017, **56**, 11080–11093.
5 J. F. Stoddart, *Angew. Chem., Int. Ed.*, 2017, **56**, 11094–11125.
6 B. L. Feringa, *Angew. Chem., Int. Ed.*, 2017, **56**, 11060–11078.
7 R. D. Astumian, *Chem. Sci.*, 2017, **8**, 840–845.
8 E. R. Kay, D. A. Leigh and F. Zerbetto, *Angew. Chem., Int. Ed.*, 2007, **46**, 72–191.
9 Y. Feng, M. Ovalle, J. S. W. Seale, C. K. Lee, D. J. Kim, R. D. Astumian and J. F. Stoddart, *J. Am. Chem. Soc.*, 2021, **143**, 5569–5591.
10 S. Kassem, T. v. Leeuwen, A. S. Lubbe, M. R. Wilson, B. L. Feringa and D. A. Leigh, *Chem. Soc. Rev.*, 2017, **46**, 2592–2621.
11 A. I. Brown and D. A. Sivak, *Chem. Rev.*, 2020, **120**, 434–459.
12 J. M. Gallagher, B. M. Roberts, S. Borsley and D. A. Leigh, *Chem*, 2024, **10**, 855–866.
13 P.-L. Wang, E. Olivieri, S. Borsley, G. F. Whitehead, A. Hasija and D. A. Leigh, *J. Am. Chem. Soc.*, 2025, **147**, 10690–10697.
14 H.-K. Liu, T. W. Mrad, A. Troncossi, S. Borsley, B. M. Roberts, A. Betts and D. A. Leigh, *J. Am. Chem. Soc.*, 2025, **147**, 8785–8795.
15 M. Baroncini, S. Silvi and A. Credi, *Chem. Rev.*, 2020, **120**, 200–268.
16 P. R. Ashton, R. Ballardini, V. Balzani, M. Gómez-López, S. E. Lawrence, M. V. Martínez-Díaz, M. Montalti, A. Piersanti, L. Prodi, J. F. Stoddart and D. J. Williams, *J. Am. Chem. Soc.*, 1997, **119**, 10641–10651.
17 V. García-López, D. Liu and J. M. Tour, *Chem. Rev.*, 2020, **120**, 79–124.
18 V. Balzani, A. Credi and M. Venturi, *Chem. Soc. Rev.*, 2009, **38**, 1542–1550.
19 D. R. S. Pooler, A. S. Lubbe, S. Crespi and B. L. Feringa, *Chem. Sci.*, 2021, **12**, 14964–14986.
20 H. Wang, H. K. Bisoyi, X. Zhang, F. Hassan and Q. Li, *Chem.–Eur. J.*, 2022, **28**, e202103906.
21 P. Roy, A. S. Sardjan, W. Danowski, W. R. Browne, B. L. Feringa and S. R. Meech, *J. Chem. Phys.*, 2024, **161**, 074504.
22 R. D. Astumian, *Proc. Nat. Acad. Sci.*, 2005, **102**, 1843–1847.
23 H. Jian and J. M. Tour, *J. Org. Chem.*, 2003, **68**, 5091–5103.
24 J. S. Seldenthuis, F. Prins, J. M. Thijssen and H. S. J. Van Der Zant, *ACS Nano*, 2010, **4**, 6681–6686.
25 Y.-L. Zhao, W. Lin, K. Jitapunkul, R. Zhao, R.-Q. Zhang and M. A. Van Hove, *ACS Omega*, 2022, **7**, 35159–35169.
26 G. Loget and A. Kuhn, *Nat. Comm.*, 2011, **2**, 535.
27 H. L. Tierney, C. J. Murphy, A. D. Jewell, A. E. Baber, E. V. Iski, H. Y. Khodaverdian, A. F. McGuire, N. Klebanov and E. C. H. Sykes, *Nat. Nanotechnol.*, 2011, **6**, 625–629.
28 D. Horinek and J. Michl, *Proc. Nat. Acad. Sci.*, 2005, **102**, 14175–14180.
29 V. Bermudez, N. Capron, T. Gase, F. G. Gatti, F. Kajzar, D. A. Leigh, F. Zerbetto and S. Zhang, *Nature*, 2000, **406**, 608–611.
30 J. Vacek and J. Michl, *Proc. Nat. Acad. Sci.*, 2001, **98**, 5481–5486.
31 G. J. Simpson, V. García-López, A. Daniel Boese, J. M. Tour and L. Grill, *Nat. Comm.*, 2019, **10**, 4631.
32 W. R. Browne and B. L. Feringa, *Annu. Rev. Phys. Chem.*, 2009, **60**, 407–428.
33 A. Guinart, Y. Qutbuddin, A. Ryabchun, J.-H. Krohn, P. Schwille and B. L. Feringa, *Chem*, 2025, 102574.
34 D. Asthana, D. Thomas, S. J. Lockyer, A. Brookfield, G. A. Timco, I. J. Vitorica-Yrezabal, G. F. Whitehead, E. J. McInnes, D. Collison, D. A. Leigh, et al., *Comm. Chem.*, 2022, **5**, 73.
35 M. Schied, D. Prezzi, D. Liu, S. Kowarik, P. A. Jacobson, S. Corni, J. M. Tour and L. Grill, *ACS Nano*, 2023, **17**, 3958–3965.
36 R. Lan, J. Bao, R. Huang, Z. Wang, L. Zhang, C. Shen, Q. Wang and H. Yang, *Adv. Mat.*, 2022, **34**, 2109800.
37 S. Borsley, D. A. Leigh and B. M. W. Roberts, *Angew. Chem., Int. Ed.*, 2024, **63**, e202400495.

38 E. Penocchio, G. Gu, A. Albaugh and T. R. Gingrich, *J. Am. Chem. Soc.*, 2025, **147**, 1063–1073.
39 T. Y. Tsong and R. Astumian, *Prog. Biophys. Mol. Bio.*, 1987, **50**, 1–45.
40 T. Y. Tsong and R. D. Astumian, *Annu. Rev. Physiol.*, 1988, **50**, 273–290.
41 R. D. Astumian, P. B. Chock, T. Y. Tsong and H. V. Westerhoff, *Phys. Rev. A*, 1989, **39**, 6416–6435.
42 R. D. Astumian and B. Robertson, *J. Am. Chem. Soc.*, 1993, **115**, 11063–11068.
43 R. D. Astumian and I. Derényi, *Eur. biophys. J.*, 1998, **27**, 474–489.
44 J. M. Bofill, W. Quapp, G. Albareda, I. de P. R. Moreira and J. Ribas-Ariño, *J. Chem. Theor. Comput.*, 2022, **18**, 935–952.
45 J. M. Bofill, W. Quapp, G. Albareda, I. de P. R. Moreira, J. Ribas-Ariño and M. Severi, *Theor. Chem. Acc.*, 2023, **142**, 22–35.
46 J. M. Bofill, M. Severi, W. Quapp, J. Ribas-Ariño, I. de P. R. Moreira and G. Albareda, *J. Chem. Phys.*, 2023, **159**, 114112.
47 J. M. Bofill, M. Severi, W. Quapp, J. Ribas-Ariño, I. de P. R. Moreira and G. Albareda, *Chem.–Eur. J.*, 2024, **30**, e202400173.
48 A. Kazaryan, J. C. M. Kistemaker, L. V. Schäfer, W. R. Browne, B. L. Feringa and M. Filatov, *J. Phys. Chem. A*, 2010, **114**, 5058–5067.
49 K. Hoki, M. Yamaki and Y. Fujimura, *Angew. Chem., Int. Ed.*, 2003, **42**, 2976–2978.
50 K. Hoki, M. Yamaki, S. Koseki and Y. Fujimura, *J. Chem. Phys.*, 2003, **119**, 12393–12398.
51 K. Hoki, M. Sato, M. Yamaki, R. Sahnoun, L. González, S. Koseki and Y. Fujimura, *J. Phys. Chem. B*, 2004, **108**, 4916–4921.
52 M. Yamaki, K. Hoki, Y. Ohtsuki, H. Kono and Y. Fujimura, *J. Am. Chem. Soc.*, 2005, **127**, 7300–7301.
53 A. Coskun, D. C. Friedman, H. Li, K. Patel, H. A. Khatib and J. F. Stoddart, *J. Am. Chem. Soc.*, 2009, **131**, 2493–2495.
54 J. A. Stroscio and D. Eigler, *Science*, 1991, **254**, 1319–1326.
55 A. C. Aragonès, N. Darwish, S. Ciampi, F. Sanz, J. J. Gooding and I. Díez-Pérez, *Nat. Comm.*, 2017, **8**, 15056.
56 S. Ciampi, N. Darwish, H. M. Aitken, I. Díez-Pérez and M. L. Coote, *Chem. Soc. Rev.*, 2018, **47**, 5146–5164.
57 H. B. Schlegel, *Theor. Chim. Acta*, 1992, **83**, 15–20.
58 W. Quapp, *Theor. Chim. Acta*, 1989, **75**, 447–460.
59 D. K. Hoffman, R. S. Nord and K. Ruedenberg, *Theor. Chim. Acta*, 1986, **69**, 265–279.
60 J. M. Bofill, W. Quapp and M. Caballero, *J. Chem. Theor. Comput.*, 2012, **8**, 927–935.
61 W. Quapp, *J. Math. Chem.*, 2018, **56**, 1339–1347.
62 F. Neese, *Wiley Interdiscip. Rev.:Comput. Mol. Sci.*, 2022, **12**, e1606.
63 A. D. Becke, *J. Chem. Phys.*, 1993, **98**, 5648–5652.
64 S. H. Vosko, L. Wilk and M. Nusair, *Can. J. Phys.*, 1980, **58**, 1200–1211.
65 C. Lee, W. Yang and R. G. Parr, *Phys. Rev. B: Condens. Matter Mater. Phys.*, 1988, **37**, 785–789.
66 F. Weigend and R. Ahlrichs, *Phys. Chem. Chem. Phys.*, 2005, **7**, 3297–3305.
67 J. Zheng, X. Xu and D. G. Truhlar, *Theor. Chem. Acc.*, 2011, **128**, 295–305.
68 S. Grimme, J. Antony, S. Ehrlich and H. Krieg, *J. Chem. Phys.*, 2010, **132**, 154104.
69 S. Grimme, S. Ehrlich and L. Goerigk, *J. Comput. Chem.*, 2011, **32**, 1456–1465.
70 F. Weigend, *Phys. Chem. Chem. Phys.*, 2006, **8**, 1057–1065.
71 R. Izsák and F. Neese, *J. Chem. Phys.*, 2011, **135**, 144105.
72 B. Helmich-Paris, B. de Souza, F. Neese and R. Izsák, *J. Chem. Phys.*, 2021, **155**, 104109.
73 M. Severi, *MANULS: A program for the electrostatic catalysis of chemical rections*, **https://github.com/MSeveri96/MANULS**.
74 T. Kudernac, N. Ruangsupapichat, M. Parschau, B. Maciá, N. Katsonis, S. R. Harutyunyan, K.-H. Ernst and B. L. Feringa, *Nature*, 2011, **479**, 208–211.
75 S. Silvi, M. Venturi and A. Credi, *J. Mater. Chem.*, 2009, **19**, 2279–2294.
76 R. D. Astumian, *Proc. Nat. Acad. Sci.*, 2007, **104**, 19715–19718.